On the level spacing distribution in quantum graphs *

F. Barra and P. Gaspard
Center for Nonlinear Phenomena and Complex Systems,
Université Libre de Bruxelles, C.P. 231,
B-1050 Brussels, Belgium

Abstract

We derive a formula for the level spacing probability distribution in quantum graphs. We apply it to simple examples and we discuss its relation with previous work and its possible application in more general cases. Moreover, we derive an exact and explicit formula for the level spacing distribution of integrable quantum graphs.

KEY WORDS: level spacing distribution, quantum graphs, ramdom matrix theory, quantum chaology, ergodicity, Poincaré surface of section.

1 Introduction

One of the major discoveries in the field of quantum chaology is the existence of universal statistical fluctuations in the spectrum of systems that are classically chaotic in the limit $\hbar \to 0$. These statistics are well described by random matrix theory (RMT) in which the Hamiltonian of the specific system under consideration is replaced by a matrix where each element is an independent random variable except for global symmetries required by the Hamiltonian [1]. Beside the universal aspects, some statistical properties may also depend on the particular system under consideration. The main tool to study all these phenomena is the Gutzwiller trace formula that gives a semiclassical approximation to the density of states in terms of the periodic orbits of the corresponding classical system [2]. The application of this formula has satisfactorily explained some statistical properties that agree with RMT for chaotic systems [3]. Nevertheless, there is no satisfactory complete explanation yet for the universal random character of the spectrum appearing from a specific Hamiltonian.

Recently, Kottos and Smilansky have studied very simple quantum systems called quantum graphs that display statistical spectral fluctuations belonging to the class of systems with a chaotic classical limit [4, 5]. A remarkable aspect of the quantum graphs is that there exists an exact trace formula that expresses

*to appear in Journal of Statistical Physics

the density of states in terms of the periodic orbits of the corresponding classical dynamics in a similar way as the Gutzwiller formula does for Hamiltonian systems. These nontrivial features of these extremely simple systems have made them natural toy models of quantum chaology.

In the same perspective, several papers have been very recently devoted to these systems [6, 7, 8, 9]. On the one hand, Kottos and Smilansky have studied scattering processes in quantum graphs showing that these systems display all the features which characterize quantum chaotic scattering [6]. On the other hand, the analysis of the statistical spectral fluctuations on graphs has been considered by Schanz and Smilansky [8] as well as by Berkolaiko and Keating [9]. These last authors have studied for star graphs the two-point correlation function, a quantity which reflects the long-range spectral correlations. In their analysis they introduce ensemble averages (for example over the lengths of the bonds) in order to get a formula which is exploited by a combinatorial analysis.

In the present article, our aim is different in two main aspects. Firstly, we want to consider the spacing probability distribution, which reflects short-range spectral correlations and, secondly, we want to study the dependence of this distribution on the parameters of the system, in particular, on the bond lengths. Accordingly, we do not introduce external average but we develop a method based on ergodicity. With this purposes, we derive a general formula for the level spacing probability distribution in quantum graphs using a very simple ergodic theorem. This formula applies more generally, too every system with levels determined by the zeros of a quasi-periodic secular equation. The result being exact, it contains all the information on the particular system. To obtain the universal behavior observed in some graphs from this result, further assumptions and simplifications should be made. We do not address here this difficult problem. Instead we apply our result to very simple graphs, which nevertheless gives interesting results (such as level repulsion) and which can guide the approach to more difficult and interesting cases.

In Section 2, we review some results about the quantum mechanics on graphs. In Section 3, we derive our main result, which is a general formula for the level spacing probability distribution given in terms of a Poincaré mapping defined in a certain surface of section Σ. In Section 4, we use the density of states for graphs to obtain information about Σ. In Section 5, we illustrate our result with some simple graphs. In Section 6, we compare the level spacing distribution obtained numerically for a complex graph, with the result of RMT. Then, in Section 7, we compare our result with a related theory proposed by Berry. Conclusions are drawn in Section 8.

2 Energy levels of quantum graphs

In this section, we introduce the main results known about the energy levels of quantum graphs in order to be complete. We refer to the works of Kottos and Smilansky for details[5].

Graphs are vertices connected by bonds. Each bond $b = (i, j)$ connects two

vertices, i and j. On each bond b, the component Ψ_b of the total wave function Ψ is a solution of the one-dimensional Schrödinger equation. Here we consider the time reversible case (*i.e.* without magnetic field)

$$-\frac{d^2}{dx^2}\Psi_b(x) = k^2\Psi_b(x), \qquad b = (i,j)\ ,$$

where k is the wavenumber. Moreover, the wave function must satisfy boundary conditions at the vertices of each bond (i and j in the previous equation), which ensures continuity and current conservation, *i.e.*,

$$\Psi_b(0) = \varphi_i$$

for all the bonds b which start at the vertex i and

$$\Psi_b(l_b) = \varphi_j$$

for all the bonds b which end in the vertex j. The length of the bond b is denoted by l_b or $l_{(i,j)}$. The current conservation reads

$$\sum{}' \frac{d}{dx}\Psi_b(x)\Big|_{x\to 0} = \lambda_i\ \varphi_i$$

where $\sum'$ denotes a summation over all the directed bonds which have their origin at the vertex i. These conditions guarantee that the resulting Schrödinger operator is self-adjoint. Note that, in this formulation, each bond has two directions and we have to distinguish between the two different directions of a bond. This means that the dimension of the vector $\Psi = [\Psi_1(x), \ldots, \Psi_{2B}(x)]^{\mathrm{T}}$ is $2B$ where B is the number of bonds of the graph.

When $\lambda_i \to \infty$ (Dirichlet boundary conditions) the graph becomes a union of noninteracting bonds. These are called "integrable graphs" because the classical dynamics corresponds to particles bouncing in the bonds leading to a phase space with the topology of a torus. We come back to this case in Subsection 5.4. For finite λ_i, the asymptotic properties of the spectrum become independent of λ at high wavenumbers and, indeed, there is a convergence to the Neumann limit where all the λ's are equal to zero. In what follows we consider this case.

As a result of the boundary conditions, we get the secular equation which can be written in the following equivalent ways

$$\det[I - S(k)] = 0 \tag{1}$$

with $S = D(k)T$ a unitary matrix of dimension $2B$ where

$$D_{ab} = \delta_{ab}\ \mathrm{e}^{ikl_a}\ , \qquad \text{with} \quad l_a = l_b \tag{2}$$

and

$$T_{ab} = -\delta_{a\hat{b}} + \frac{2}{v^i} \tag{3}$$

if the bonds a and b are connected through a vertex (here called i) and zero otherwise. The notation $\hat{b}$ defines the reverted b bond.

The secular equation can also be written as

$$\det h(k) = 0$$

where h is a matrix of dimension V (V is the number of vertices in the graph) given by

$$h_{ij}(k) = \begin{cases} -\sum_{m \neq i} \cot k l_{(i,m)} C_{im} & \text{if } i = j \\ (\sin k l_{(i,j)})^{-1} C_{ij} & \text{if } i \neq j \end{cases} \tag{4}$$

C_{ij} being the connectivity matrix with elements equal to one if the vertex i is connected to j and zero otherwise.

It is clear from both secular equations that the eigenvalues are given by the zeros of an almost-periodic function.

Using Eqs. (1), (2), and (3), it is possible to write the quantization condition in terms of the zeta function

$$\zeta(k) = \prod_p \left[1 - \mathrm{e}^{-\frac{\gamma_p}{2} n_p} \ \mathrm{e}^{i(kL_p + \mu_p \pi)}\right] = 0$$

where p denotes a periodic orbit, n_p is its period, L_p is its length, γ_p is related to the stability of the orbit and μ_p is the analogue of the Maslov index. Note that $L_p = \sum_i m_i l_i$ where the m_i are integer numbers. If we define $x_i = k l_i$ we can see that $\zeta(k) = \zeta(x_1 = k l_1, \ldots, x_B = k l_B)$ with

$$\zeta(x_1, \ldots, x_B) = \prod_p \left[1 - \mathrm{e}^{-\frac{\gamma_p}{2} n_p} \ \mathrm{e}^{i\left(\sum_i m_i x_i + \mu_p \pi\right)}\right] \tag{5}$$

Note that $\zeta(x_1, \ldots, x_B)$ is 2π-periodic in each of the variables, so that $\zeta(k)$ is an almost-periodic function. It can happen that the lengths of the graph are not all incommensurate. In that case, it is convenient to define a new function $F(x_1, \ldots, x_n)$ where n is the number of incommensurate lengths, which gives $\zeta(k)$ when evaluated in $x_1 = k l_1, \ldots, x_n = k l_n$ (here $l_1, \ldots, l_n$ are the incommensurate lengths) , *i.e.*,

$$F(x_1 = k l_1, \ldots, x_n = k l_n) = f(k) = \zeta(k)$$

3 Level spacing distribution for almost-periodic functions

3.1 The level spacings as the first-return times of a Poincaré mapping

In this section, we derive the probability distribution for the spacing between the successive zeros of an almost-periodic function $f(k)$. Let us call $\{k_l\}_{l=0}^{\infty}$ the ordered solutions of $f(k) = 0$.

The probability of having two successive zeros at a distance $(s, s+ds)$ is given by

$$P(s)ds = \lim_{K\to\infty} \frac{\#\{k_l \leq K : s \leq k_{l+1} - k_l \leq s + ds\}}{\#\{k_l \leq K\}}$$

or equivalently by

$$P(s) = \lim_{N\to\infty} \frac{1}{N} \sum_{l=0}^{N-1} \delta[s - (k_{l+1} - k_l)] \tag{6}$$

By the definition of $f(k)$, there exists a function $F(x_1, x_2, ..., x_n)$ such that

$$f(k) = F(x_1 = kl_1, x_2 = kl_2, ..., x_n = kl_n)$$

where the parameters $l_1, l_2, ..., l_n$ are incommensurate real numbers, which, for the case of graphs, form the set of incommensurate lengths, and from which all the other lengths can be obtained by linear combinations with rational coefficients.

The function $F(x_1, x_2, ..., x_n)$ is periodic in each of its arguments x_i with a prime period P_i. Accordingly, we can consider the function F on a torus $T^n : 0 \leq x_i \leq P_i$ with $i = 1, ...n$.

The equation

$$F(x_1, x_2, ..., x_n) = 0 \tag{7}$$

defines a hypersurface Σ on T^n.

The equations

$$\frac{dx_i}{dk} = l_i \qquad (i = 1, \ldots, n) \tag{8}$$

define a flow on this torus. In Eq. (8), the wavenumber k plays the role of the time. Because of the incommensurability of the "frequencies" l_i this flow has the remarkable property of being ergodic. We will exploit this property of dynamical systems theory to obtain the desired expression for the level spacing probability distribution.

First, we note that each intersection of the trajectory $\{x_i = kl_i\}_{i=1}^n$with the surface Σ gives a zero $k_j \in \{k_l\}_{l=0}^\infty$. Therefore, this surface plays the role of a Poincaré surface of section for the present dynamical system.

In this hypersurface of section, the flow induces a Poincaré map

$$\left\{ \begin{array}{lcl} \xi_{n+1} & = & \phi(\xi_n) \\ k_{n+1} & = & k_n + \tau(\xi_n) \end{array} \right. \tag{9}$$

where ξ_n is a point on Σ that is mapped by the flow on ξ_{n+1} also in Σ. These two points are the successive intersections of the trajectory $\{x_i = kl_i\}_{i=1}^n$ with the surface Σ at the times k_n and k_{n+1} respectively. $\tau(\xi)$ is the time of first return to the surface of section Σ.

From Eqs. (9), we have that

$$k_{n+1} - k_n = \tau[\phi^n(\xi_0)]$$

in which ξ_0 is an initial condition belonging to Σ where the iteration started.

Now, we can write the spacing probability distribution (6) in the form

$$P(s) = \lim_{N\to\infty} \frac{1}{N} \sum_{l=0}^{N-1} \delta\left\{s - \tau[\phi^l(\xi_0)]\right\} \tag{10}$$

The ergodicity implies that the value of the distribution (10) is almost everywhere independent of the initial condition ξ_0, so that ξ_0 can be any point on the torus T^n and not necessary one corresponding to a zero. Moreover, the ergodicity implies the existence of a measure ν on Σ which gives the spacing probability distribution according to

$$P(s) = \int_\Sigma \nu(d\xi)\ \delta[s - \tau(\xi)] \tag{11}$$

We now turn to the determination of this invariant measure ν.

3.2 The invariant measure ν

When the lengths l_i are incommensurate, the dynamical system (8) is ergodic on the torus. That is: For any measurable function $g(x_1, ..., x_n)$ defined on the torus we have that

$$\lim_{T\to\infty} \frac{1}{T} \int_0^T g[\varphi^t(x_0)]\ dt = \int_{T^n} \mu(dx)\ g(x) \tag{12}$$

where $\varphi^t(x_0) = lt + x_0$ is the flow (φ^t, l and x_0 are n-dimensional vectors) and $\mu(dx) = \frac{dx}{|T^n|}$ is the Lebesgue measure on the torus.

Let us define the function $\Delta t[\varphi^t(x_0)]$ as the time of flight of the trajectory after the last crossing of the surface of section Σ. If the last crossing happened at k_n then $\Delta t[\varphi^t(x_0)] = t - k_n$.

We replace the function g by

$$g[\varphi^t(\xi_0)] = \Theta\left\{s - \Delta t[\varphi^t(\xi_0)]\right\} \sum_{\{n\}} \delta(t - k_n) \tag{13}$$

and we compute in this case the integral of the left-hand side of Eq. (12)

$$\int_0^T g[\varphi^t(\xi_0)]\ dt = \sum_{\{n\}} \int_0^T \Theta\left\{s - \Delta t[\varphi^t(\xi_0)]\right\}\ \delta(t - k_n)\ dt$$

We assume that there are N zeros in the interval $[0, T]$ and we call them $k_0, ..., k_{N-1}$ so that we get

$$\int_0^T g[\varphi^t(\xi_0)]\ dt = \sum_{n=0}^{N-1} \Theta[s - (k_{n+1} - k_n)] = \sum_{n=0}^{N-1} \Theta\left\{s - \tau[\phi^n(\xi_0)]\right\}$$

For large values of T we can consider that $T = k_N$ with N the number of zeros. Denoting by $\langle d \rangle$ the mean density of zeros, we have $N = \langle d \rangle \, k_N$ and $T = \frac{N}{\langle d \rangle}$ so that we finally get

$$\lim_{T\to\infty} \frac{1}{T} \int_0^T g[\varphi^t(\xi_0)] \; dt = \langle d \rangle \lim_{N\to\infty} \frac{1}{N} \sum_{n=0}^{N-1} \Theta \left\{ s - \tau[\phi^n(\xi_0)] \right\} \tag{14}$$

We recognize the cumulative function times the mean density in the right-hand side of the expression (14).

To compute the right-hand side of Eq. (12), we have to write g as a function of the coordinates x. For this purpose, we remember that

$$\sum_{\{n\}} \delta(t - k_n) = |f'(t)| \, \delta[f(t)] \; . \tag{15}$$

Now $f(t) = F[\varphi^t(\xi_0)]$ and $f'(t) = \nabla F[\varphi^t(\xi_0)] \cdot l$. Replacing these expressions in (15), and (15) in (13), we obtain

$$g[\varphi^t(\xi_0)] = \Theta \left\{ s - \Delta t[\varphi^t(\xi_0)] \right\} \; \left| \nabla F[\varphi^t(\xi_0)] \cdot l \right| \; \delta \left\{ F[\varphi^t(\xi_0)] \right\}$$

from which we infer

$$g(x) = \Theta[s - \Delta t(x)] \; \left| \nabla F(x) \cdot l \right| \; \delta[F(x)]$$

where $\Delta t(x)$ is the time taken by the trajectory to arrive at x since its last crossing with Σ.

Now, we compute the right-hand side of Eq. (12) which we denote by I:

$$I = \int_{T^n} \mu(dx) \; g(x) = \frac{1}{|T^n|} \int_{T^n} dx \; g(x) \tag{16}$$

We perform the nonlinear change of coordinates $x \to (t, \xi)$ where ξ are the $n-1$ coordinates that parametrize the surface Σ, *i.e.*

$$x_i = l_i t + s_i(\xi) \tag{17}$$

where the functions $s_i(\xi)$ are such that $F[s_1(\xi), ..., s_n(\xi)] = 0$. In the new coordinates, the equation for the surface Σ is $t = 0$ or $t = \tau(\xi)$. In these new coordinates, we have that

$$\Delta t(x) = t \tag{18}$$

$$dx = J(\xi) \; d\xi \; dt \tag{19}$$

with the Jacobian determinant

$$J(\xi) = \begin{vmatrix} l_1 & \cdots & l_n \\ \frac{\partial s_1}{\partial \xi_1} & \cdots & \frac{\partial s_n}{\partial \xi_1} \\ \vdots & \ddots & \vdots \\ \frac{\partial s_1}{\partial \xi_{n-1}} & \cdots & \frac{\partial s_n}{\partial \xi_{n-1}} \end{vmatrix} \tag{20}$$

and $0 \leq t \leq \tau(\xi)$ where $\tau(\xi)$ is the time of first return previously introduced. In these coordinates, I is given by

$$I = \frac{1}{|T^n|} \int_\Sigma d\xi \; J(\xi) \int_0^{\tau(\xi)} dt \; \Theta(s-t) \; |\nabla F \cdot l| \; \delta[F(\xi,t)]$$

The integration over t can be carried out using a new variable u defined through

$$u(t) = F(\xi, t) \tag{21}$$

where ξ is kept constant. Differentiating with respect to t gives $\frac{du}{dt} = \nabla F \cdot l$ and we get

$$I = \frac{1}{|T^n|} \int_\Sigma d\xi \; J(\xi) \int \frac{du}{|\nabla F \cdot l|} \; \Theta[s - t(u)] \; |\nabla F \cdot l| \; \delta(u)$$

This integral picks up the value of $t(u)$ at $u = 0$. From Eq. (21), we see that $u = 0$ is the equation that defines Σ and, as we noticed after Eq. (17), there are two solutions $t(0) = 0$ or $t(0) = \tau(\xi)$ in the new coordinates. But since t is the "time of flight" after the last crossing, we consider the second solution and we finally get

$$I = \frac{1}{|T^n|} \int_\Sigma d\xi \; J(\xi) \; \Theta[s - \tau(\xi)] \; . \tag{22}$$

From Eqs. (12), (14), (16), and (22), we find the cumulative function and by differentiation with respect to s we obtain the level spacing probability density

$$P(s) = \lim_{N\to\infty} \frac{1}{N} \sum_{n=0}^{N-1} \delta\left\{s - \tau[\phi^n(\xi_0)]\right\} = \frac{1}{\langle d \rangle \, |T^n|} \int_\Sigma d\xi \; J(\xi) \; \delta[s - \tau(\xi)] \tag{23}$$

On the other hand, the density can also be expressed in a geometrical form. Indeed, starting from its definition

$$\langle d \rangle = \lim_{T\to\infty} \frac{\#\{k_n < T\}}{T} = \lim_{T\to\infty} \frac{1}{T} \int_0^T \sum_{\{l\}} \delta(t - k_n) \; dt$$

and using Eq. (15) and Eq. (12), we have

$$\langle d \rangle = \frac{1}{|T^n|} \int_{|T^n|} dx \; |\nabla F \cdot l| \; \delta[F(x)]$$

Rewriting this expression in terms of the new coordinates (17) and then doing the changes of variables (21), we obtain

$$\langle d \rangle = \frac{1}{|T^n|} \int_\Sigma d\xi \; J(\xi) \tag{24}$$

Let us observe that this expression (24) for the density can be obtained directly from Eq. (23) and the normalization condition $\int_0^\infty P(s)ds = 1$.

Accordingly, we can write the spacing probability density as

$$P(s) = \frac{\int_\Sigma d\xi \ J(\xi) \ \delta[s - \tau(\xi)]}{\int_\Sigma d\xi \ J(\xi)} \tag{25}$$

which is the central result of this paper. The expression (25) has a very simple geometrical interpretation. It gives the spacing probability density as the ratio between the flux of the probability current $l\delta[s - \tau(\xi)]$ through the surface Σ and the flux of the constant velocity field l through the same surface Σ.

From Eq. (25), we can conclude that the invariant measure ν in (11) is given by

$$\nu(d\xi) = \frac{d\xi \ J(\xi)}{\int_\Sigma d\xi \ J(\xi)} \ .$$

4 The density of states as a sum rule for graphs

In the previous section, we derived a formula which relates the density of zeros of an almost-periodic function to the properties of the surface of section Σ defined in a torus. The dimension of the torus equals the number of incommensurate lengths and the periodicity P_i in each variable depends on the relations between the length l_i and those which are commensurable with it. For example, if there is a length commensurable with l_1, *i.e.*, $l_k = \frac{p}{q} l_1$ then the variable x_1 will have the period $P_1 = 2\pi q$. In the case where the relation is of the form $l_k = nl_1$, or all the lengths are incommensurable, we can always consider that $P_i = 2\pi$, $\forall i$. In what follows, we consider this to be the case. As a consequence, we can rewrite Eq. (24) as

$$\langle d \rangle = \frac{1}{(2\pi)^n} \int_\Sigma d\xi \ J(\xi) \tag{26}$$

As we have already pointed out, this expression has the geometrical interpretation of a constant flux l through the surface Σ. Because of the periodicity of Σ in the n-dimensional real space R^n, we expect that the projection of Σ in all of the n directions covers the complete plane. (This would be false if Σ was a closed surface but we suppose that this is not the case.) Therefore, if we call Σ_i the projection of Σ in the i^{th} direction we have

$$\langle d \rangle = \frac{1}{(2\pi)^n} \int_\Sigma d\xi \ J(\xi) = \frac{1}{(2\pi)^n} \sum_i l_i \int_{\Sigma_i} ds_i$$

and $\int_{\Sigma_i} ds_i = m_i (2\pi)^{n-1}$ with m_i the number of sheets of Σ for the projection in the i^{th} direction. Consequently, we have

$$\langle d \rangle = \frac{1}{2\pi} \sum_i m_i \ l_i. \tag{27}$$

The number m_i can be determined for each particular case by inspection on the quantization formula [for example Eq. (1)].

Here, our purpose is to revert the argument and use this formula to obtain the m_i. This is possible because there is a general expression for the density. For graphs, the density of states was obtained in Ref. [5] using the properties of (1), (2) and (3) together with a formula for the density of states derived in the approach of scattering quantization. The result is simply given by

$$\langle d \rangle = \frac{L_{\rm tot}}{\pi} \ . \tag{28}$$

From Eqs. (27)-(28), we get the desired equation for the m_i's

$$\sum_i m_i \ l_i = 2L_{\rm tot} \tag{29}$$

Since the sum is only performed over the incommensurate lengths, forming a basis from which all other lengths can be obtained, this equation gives all the m_i because we can write $L_{\rm tot}$ in such a basis.

We can deduce from here that when all the lengths are incommensurable there will be two sheets in each projection.

It is possible to reduce the "volume" of the torus by noticing that, in fact, we do not need the function $F(x_1, \ldots, x_n)$ to be periodic but the surface Σ. Since this surface is given by $F(x_1, \ldots, x_n) = 0$, the period P_i with which the surface is repeated in R^n is given by the smallest of the period or anti-period of the function in the variable x_i [*i.e.*, the values P_i for which $F(x_1, \ldots, x_i + P_i, \ldots, x_n) = \pm F(x_1, \ldots, x_i, \ldots, x_n)$]. Note that we call it again P_i but there is no risk of confusion. Moreover, in the rest of the paper, we shall use this definition.

5 Application to simple systems

5.1 A three-bond star graph with three different bond lengths

Let us consider the simple graph composed by three bonds attached to a vertex. The spectrum of this graph is given by the zeros of the function

$$f(k) = \cos kl_1 \cos kl_2 \sin kl_3 + \cos kl_1 \sin kl_2 \cos kl_3 + \sin kl_1 \cos kl_2 \cos kl_3 \tag{30}$$

The function (30) is an almost-periodic function. Let us define

$$G(x_1, x_2, x_3) = \cos x_1 \cos x_2 \sin x_3 + \cos x_1 \sin x_2 \cos x_3 + \sin x_1 \cos x_2 \cos x_3$$

This function is 2π-periodic in each argument but has an anti-period π. It satisfies

$$G(x_1 = kl_1, x_2 = kl_2, x_3 = kl_3) = f(k)$$

The equation $G(x_1, x_2, x_3) = 0$ defines a surface Σ with a double cone joined by a singular point. The singular point is given by $x_1 = \frac{\pi}{2}, x_2 = \frac{\pi}{2}, x_3 = \frac{\pi}{2}$ (see Fig. 1). For simplicity, we translate the coordinate system to that point so that we consider the function

$$F(x_1, x_2, x_3) = G\left(x_1 - \frac{\pi}{2}, x_2 - \frac{\pi}{2}, x_3 - \frac{\pi}{2}\right)$$

defined on the torus $-\frac{\pi}{2} < x_i \leq \frac{\pi}{2}$.

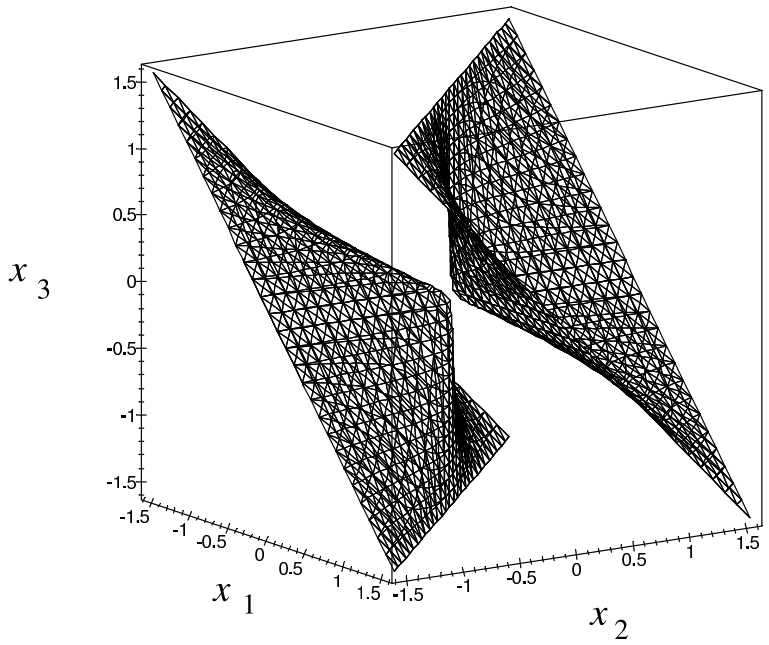

Figure 1: Plot of the surface Σ for the three-bond star graph with three different lengths. The plot is obtained from $G(x_1, x_2, x_3) = 0$.

As we saw in Section 3, the shape of the surface Σ determines the level spacing probability distribution. For small spacings s, the distribution is given by the iterations with short "times of flight". These are determined by intersections near the singularity of Σ because there are arbitrarily close points in its neighborhood. In order to study the behavior of the level spacing probability distribution for small spacings we carry out our analysis near the singular point where the function F can be approximated by the quadratic function

$$F(x_1, x_2, x_3) = x_1x_2 + x_1x_3 + x_2x_3 + \mathcal{O}(x_i^3)$$

We diagonalize the quadratic form with a rotation of coordinates and we finally get

$$F(y_1, y_2, y_3) = 2y_1^2 - y_2^2 - y_3^2 + \mathcal{O}(y_i^3). \tag{31}$$

In the y-coordinates, the flow is given by $\frac{dy_i}{dk} = e_i$ where $e_1 = (l_1 + l_2 + l_3)/\sqrt{3}$, $e_2 = (l_2 - l_3)/\sqrt{2}$, $e_3 = (l_2 + l_3 - 2l_1)/\sqrt{3}$. Now, we apply our theory. We define new coordinates through the transformation $(y_1, y_2, y_3) \to (\eta, \xi, t)$

$$\begin{aligned} y_1 &= s_1(\eta, \xi) + e_1 t \\ y_2 &= s_2(\eta, \xi) + e_2 t \\ y_3 &= s_3(\eta, \xi) + e_3 t \end{aligned} \tag{32}$$

where the functions $s_i(\eta, \xi)$ are zeros of Eq. (31), *i.e.*, $2s_1^2 - s_2^2 - s_3^2 = 0$. A solution is

$$\begin{aligned} s_1(\eta, \xi) &= -\sqrt{\frac{\eta^2 + \xi^2}{2}} \\ s_2(\eta, \xi) &= \eta \\ s_3(\eta, \xi) &= \xi \end{aligned} \tag{33}$$

Eqs. (32) and (33) define the new variables. We need to compute J and $\tau(\eta, \xi)$. For J, the calculation is straightforward. Using (20) and (33), we get

$$J = \left| \frac{b(\eta, \xi)}{\sqrt{2(\eta^2 + \xi^2)}} \right| \tag{34}$$

where

$$b(\eta, \xi) = 2e_1 s_1 - e_2 s_2 - e_3 s_3 = -\left[e_1 \sqrt{2(\eta^2 + \xi^2)} + e_2 \xi - e_3 \eta \right] + \mathcal{O}(2) \tag{35}$$

The notation $\mathcal{O}(2)$ means here "to second order in η, ξ or t". If we write Eq. (31) in the new coordinates we get

$$F(\eta, \xi, t) = \alpha^2 t^2 + 2\ t\ b(\eta, \xi) + (2s_1^2 - s_2^2 - s_3^2) + \mathcal{O}(3) \tag{36}$$

where b is defined by Eq. (35) and

$$\alpha^2 = 2e_1^2 - e_2^2 - e_3^2 = 2(l_1 l_2 + l_2 l_3 + l_1 l_3) \tag{37}$$

The third term in Eq. (36) is zero by definition. In the new coordinates, the surface of section Σ is given by the roots of $F(\eta, \xi, t) = 0$, *i.e.*, $t = 0$ and $t = -\frac{2b}{\alpha^2}$. The function $\tau(\eta, \xi)$ represents the "time of flight" of a trajectory which starts at one point on the lower cone with coordinates (η, ξ) and arrives to the upper cone. That is

$$\tau(\eta, \xi) = -\frac{2b}{\alpha^2} = \frac{2\left[\sqrt{2(\eta^2 + \xi^2)} + e_2 \xi - e_3 \eta \right]}{2e_1^2 - e_2^2 - e_3^2} + \mathcal{O}(2) \tag{38}$$

Now we are ready to compute $P(s)$ for small s using (25). As we have already noticed the integral in the denominator is just the density of states which is

$$\langle d \rangle = \frac{l_1 + l_2 + l_3}{\pi} \tag{39}$$

for this graph. The integral in the numerator is

$$I = \int d\xi \; d\eta \; \frac{|b(\xi,\eta)|}{\sqrt{2(\xi^2+\eta^2)}} \; \delta\left(s + \frac{2b}{\alpha^2}\right) + \mathcal{O}(s^2)$$

which is performed by changing to a variable $u(\xi) = s + \frac{2b}{\alpha^2}$ where η is kept constant, by using (38), and then by integrating in η. The details of this calculation are left to the reader. The result is

$$I = \left(\frac{\alpha}{2}\right)^{\frac{3}{2}} \frac{s}{\pi^2} + \mathcal{O}(s^2)$$

This, together with (37) and (39), gives

$$P(s) = \frac{(l_1 l_2 + l_1 l_3 + l_2 l_3)^{\frac{3}{2}}}{l_1 + l_2 + l_3} \frac{s}{\pi} + \mathcal{O}(s^2)$$

Usually, we express this probability density in the scaled variable Δ such that the mean level spacing is equal to unity:

$$P(\Delta) = \pi \frac{(l_1 l_2 + l_1 l_3 + l_2 l_3)^{\frac{3}{2}}}{(l_1 + l_2 + l_3)^3} \Delta + \mathcal{O}(\Delta^2) \tag{40}$$

We observe that this simple graph already presents the Wignerian level repulsion, a property usually associated to chaotic classical dynamics. To our knowledge, there are only a few systems for which this result can be derived exactly.

In Fig. 2, the cumulative function is depicted as a function of Δ^2 and compared with a numerical calculation of the spacing distribution. The slope at the origin is half of the slope of $P(\Delta)$. The straigth line in the figure has half of the slope given by (40). We see that there is very good agreement between (40) and the numerical result.

There is an interesting point about this result. The slope of (40) takes values between zero and $\frac{\pi}{3^{\frac{3}{2}}} \sim 0.6$ as the lengths l_1, l_2, l_3 vary. Therefore, the slope only varies on a relatively small interval. This means that changing the length of the bonds (but always keeping them irrationally related) does not change very much the slope of the spacing probability density $P(\Delta)$. Moreover, we note that the dependence on the lengths can be seen as a quotient between two different averages of the lengths (a geometric average and a arithmetic one).

It is also interesting to notice in Fig. 1 that the projections of the surface Σ onto each axis cover the corresponding plane only once in the torus of volume π^3, which is implied by the formula (29) of Section 4 and by Eq. (39).

5.2 A three-bond star graph with two different bond lengths

Now, we consider the same graph as in the previous subsection but with only two different lengths, say l_1, l_2. Taking $l_1 = l_3$ in (30), we get the function which gives the zeros for this graph

$$f(k) = \cos kl_1 \, (2 \sin kl_1 \cos kl_2 + \sin kl_2 \cos kl_1)$$

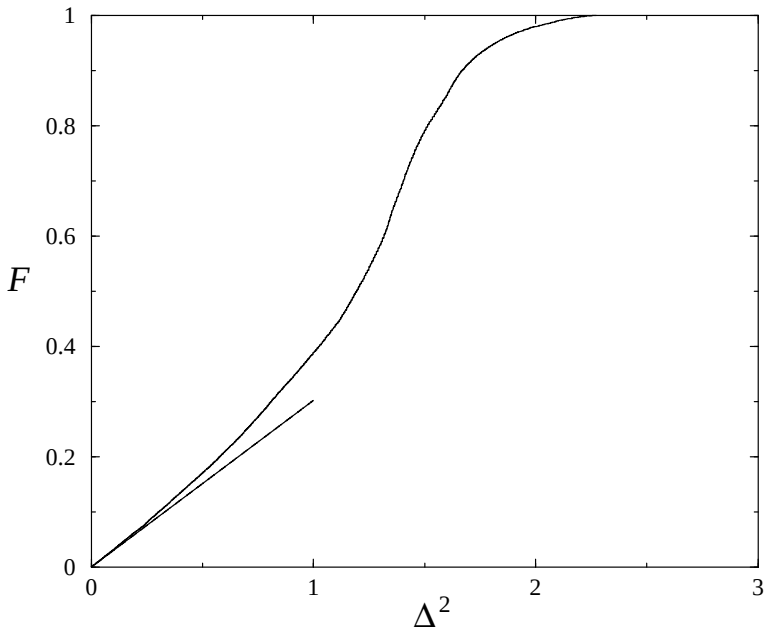

Figure 2: Plot of the cumulative function $F = \int_0^\Delta P(\Delta')d\Delta'$ of the level spacing distribution, as a function of Δ^2 for the three-bond star graph. The straight line is the prediction obtained by integration of Eq. (40). Here, $l_1 = \pi$, $l_2 = 3.183459012$, and $l_3 = 3.1442336073$.

We now introduce the function

$$F(x_1, x_2) = \cos x_1 \, (2 \sin x_1 \cos x_2 + \sin x_2 \cos x_1)$$

such that $F(x_1 = kl_1, x_2 = kl_2) = f(k)$. The function $F(x_1, x_2)$ is π periodic in x_1 and π anti-periodic in x_2 and can be considered in the torus $0 < x_i \leq \pi$ with $i = 1, 2$. In Fig. 3, we draw the lines where $F(x_1, x_2) = 0$ in the plane (x_1, x_2). Changing the origin of the coordinates to the singular point $(\frac{\pi}{2}, \frac{\pi}{2})$ corresponds to analyze the function

$$G(x_1, x_2) = -\sin x_1 \, (2 \sin x_2 \cos x_1 + \sin x_1 \cos x_2)$$

Note that around the singularity the function G can be approximated by the quadratic form $2x_1x_2 + x_1^2$. In this example, we explicitly obtain the density of states using $\langle d \rangle = \frac{1}{\pi^n} \int_\Sigma J \, d\xi$. First, we identify the surface Σ as the union of two lines Σ_1 and Σ_2 as indicated in Fig. 3 so that

$$\langle d \rangle = \frac{1}{\pi^2} \left(\int_{\Sigma_1} J \, d\xi + \int_{\Sigma_2} J \, d\xi \right)$$

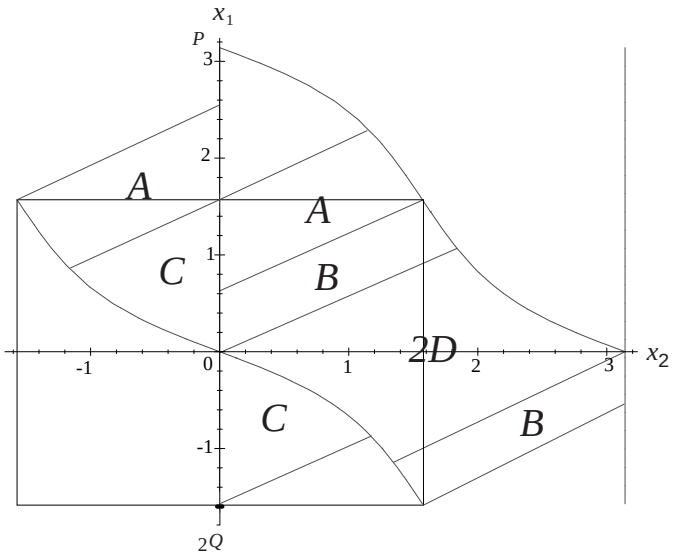

Figure 3: Schematic representation of the torus for the problem of Subsection 5.2. The surface Σ is composed of the x_1-axis and of the curved curve. The trajectories that cross the surface Σ belong to the region A, B, C or D. Note in the figure that the regions D are one next to each other that is why we put $2D$.

where Σ_1 is given by $\sin x_1 = 0$, *i.e.*, $\Sigma_1 = \{x_1 = 0, -\frac{\pi}{2} < x_2 < \frac{\pi}{2}\}$. This surface is given by $s_1(\xi) = 0$ and $s_2(\xi) = \xi$ so that $J = \begin{vmatrix} l_1 & l_2 \\ \frac{ds_1}{d\xi} & \frac{ds_2}{d\xi} \end{vmatrix} = l_1$. The surface Σ_2 is given by $2\sin x_2 \cos x_1 + \sin x_1 \cos x_2 = 0$, *i.e.*, $x_2 = -\arctan\left(\frac{1}{2}\tan x_1\right)$. Therefore, if $s_1(\xi) = \xi$ we find $s_2(\xi) = -\arctan\left(\frac{1}{2}\tan\xi\right)$ so that we get $J = \left|l_2 + \frac{2l_1}{1+\cos^2\xi}\right|$. Consequently, we obtain

$$\langle d \rangle = \frac{1}{\pi^2}\left[\int_{-\frac{\pi}{2}}^{\frac{\pi}{2}} l_1 \, d\xi + \int_{-\frac{\pi}{2}}^{\frac{\pi}{2}} \left(l_2 + \frac{2l_1}{1+\cos^2\xi}\right) \, d\xi\right] = \frac{2l_1 + l_2}{\pi}$$

as expected. In Fig. 3, we notice that there are two sheets of Σ with projection onto x_2 and only one with projection onto x_1 as expected from the formula (29) of Section 4.

Let us compute the level spacing probability density $P(s)$. From the symmetry of Fig. 3, we recognize four regions (A, B, C, D), each one repeated twice. For three of these regions (A, B, C), a trajectory joins a straight line with a curved one. For the other region (D), two curved lines are joined. In this respect, we need two expressions for the "time of flight": $\tau_1(\xi)$ and $\tau_2(\xi)$.

The "surface of arrival" is determined by $2\sin x_2 \cos x_1 + \sin x_1 \cos x_2 = 0$,

i.e., $x_2 = -\arctan\left(\frac{1}{2}\tan x_1\right)$. Considering $x_2 = l_2 t + \xi$ and $x_1 = l_1 t$, we get

$$\xi = -l_2 t - \arctan\left[\frac{1}{2}\tan(l_1 t)\right] \tag{41}$$

Solving this equation for $t = t(\xi)$, we find that $\tau_1(\xi) = |\min t(\xi)|$. From the periodicity of the arctangent function, the next solution [let us call it $t_2(\xi)$] gives the time to cross the following surface (see Fig. 3) so that $\tau_2(\xi) = t_2(\xi) - \tau_1(\xi)$. Since the parameter ξ moves in the x_2-axis, we can write

$$\int_\Sigma J\ \delta[s-\tau(\xi)]\ d\xi = 2l_1 \int_0^P \delta[s-\tau_1(\xi)]\ d\xi + 2l_1 \int_Q^0 \delta[s-\tau_2(\xi)]\ d\xi$$

where $P = \pi$ and $Q = -\frac{l_2\pi}{2l_1}$. The first integral takes the contributions from the regions (A, B, C) and is easy to compute with the change of variable $u = \tau_1(\xi)$. We find

$$\int_0^P \delta[s-\tau_1(\xi)]\ d\xi = \int_0^{\tau_P} \frac{du}{\left|\frac{d\tau_1[\xi(u)]}{d\xi}\right|}\ \delta(s-u)$$

where $\tau_P = \frac{\pi}{l_1} - \tau_1(\frac{l_2\pi}{l_1})$. Differentiating (41) with respect to ξ, we get

$$\left|\frac{d\tau_1[\xi(u)]}{d\xi}\right| = \frac{1}{\left|l_2 + \frac{2l_1}{1+\cos^2 u}\right|}$$

so that

$$\int_0^{\tau_P} \delta[s-\tau_1(\xi))]\ d\xi = \begin{cases} \left|l_2 + \frac{2l_1}{1+3\cos^2 l_1 s}\right|\ , & \text{for} \quad s < \tau_P \\ 0\ , & \text{for} \quad s > \tau_P \end{cases}$$

For the second integral which takes the contribution of the region D, we have a similar formula but it depends on the implicit functions $\tau_1(\xi)$ and $\xi(s)$ given by the equation $\tau_2(\xi) = s$. If $\tau_2(Q) \equiv \frac{\pi}{l_1} - 2\tau_1(-\frac{l_2\pi}{2l_1}) < s < \tau_P$ we get

$$\int_Q^0 \delta[s-\tau_2(\xi)]\ d\xi = \left|\left\{l_2 + \frac{2l_1}{1+3\cos^2 l_1[s+\tau_1(\xi(s))]}\right\}^{-1} + \left\{l_2 + \frac{2l_1}{1+3\cos^2 l_1[\tau_1(\xi(s))]}\right\}^{-1}\right|^{-1}$$

and zero if $s > \tau_P$. Hence, in the scaled variable $\Delta = \frac{L_{\rm tot}}{\pi}s$, we have

$$P(\Delta) = \frac{2l_1}{L_{\rm tot}^2}\left|l_2 + \frac{2l_1}{1+3\cos^2 l_1 \Delta\frac{\pi}{L_{\rm tot}}}\right| + \frac{2l_1}{L_{\rm tot}^2}\Gamma(\Delta) \tag{42}$$

where $\Gamma(\Delta) = 0$ if $\Delta < \frac{L_{\rm tot}}{\pi}\tau_2(Q)$ and

$$\Gamma(\Delta) = \left|\frac{1}{l_2 + \frac{2l_1}{1+3\cos^2 l_1\left\{\frac{\pi\Delta}{L_{\rm tot}} + \tau_1[\xi(\Delta\frac{\pi}{L_{\rm tot}})]\right\}}} + \frac{1}{l_2 + \frac{2l_1}{1+3\cos^2 l_1\left\{\tau_1[\xi(\Delta\frac{\pi}{L_{\rm tot}})]\right\}}}\right|^{-1} \tag{43}$$

if $\frac{L_{\rm tot}}{\pi}\tau_2(Q) < s < \frac{L_{\rm tot}}{\pi}\tau_P$. Finally, we note that $P(\Delta) = 0$ if $\Delta > \frac{L_{\rm tot}}{\pi}\tau_P$.

The fact that $\Gamma(\Delta)$ has an implicit dependence on Δ, makes difficult its actual evaluation. Nevertheless, in the numerical example considered below, the interval $\frac{L_{\rm tot}}{\pi}\tau_2(Q) < s < \frac{L_{\rm tot}}{\pi}\tau_P$ where $\Gamma(\Delta)$ is different from zero is small and we can consider a simple approximation for $\Gamma(\Delta)$.

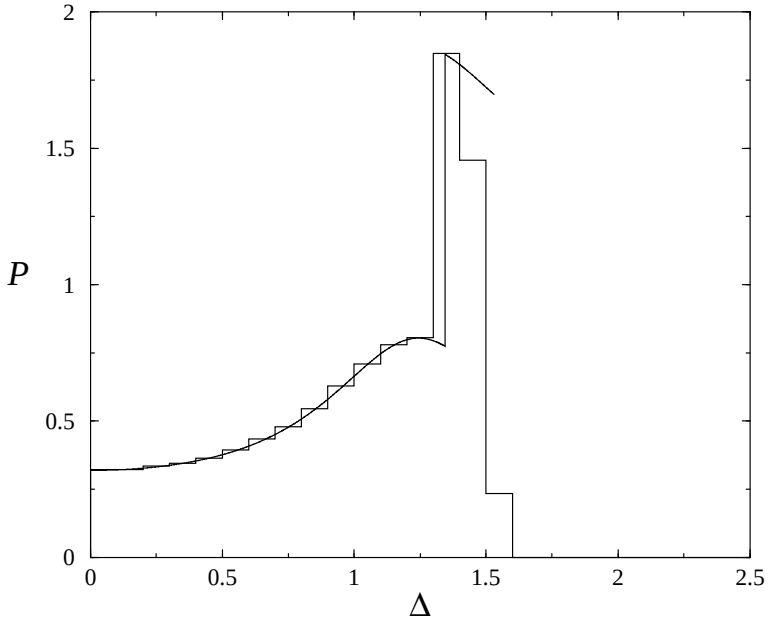

Figure 4: Numerical and theoretical level spacing probability densities for the graph of 3 bonds with 2 different lengths, $l_1 = \pi$ and $l_2 = 1.53183459$.

Consider $l_1 = \pi$ and $l_2 = 1.53183459012$. Thus, we get $\frac{L_{\rm tot}}{\pi}\tau_2(Q) = 1.345$ and $\frac{L_{\rm tot}}{\pi}\tau_P = 1.522$. Therefore, $\Gamma(\Delta)$ is different from zero in the interval $1.345 < \Delta < 1.522$ as can be observed in Fig. 4. In this interval, we can consider $\tau_2(\xi)$ as a linear function of ξ (from Fig. 3 we see that the dependence on ξ is in fact smooth). Accordingly, $\Gamma(\Delta)$ is simply given by the constant $\frac{Q}{\tau_2(Q)-\tau_p}$. [Remember that $Q = -\frac{l_2\pi}{2L_{\rm tot}}$. See after Eq. (41).] Subtituting the numerical values, we get $\frac{2l_1}{L_{\rm tot}^2}\Gamma = 1.107$ which added to the first term of Eq. (42) predicts a peak of the order of 1.8, which agrees with the peak of the numerical result shown in Fig. 4. A more accurate comparison can be done through the cumulative function $F(\Delta) = \int_0^\Delta d\Delta' P(\Delta')$. Fig. 5 shows the numerical result and the analytical result obtained by integration of Eq. (42) using the approximation $\frac{2l_1}{L_{\rm tot}^2}\Gamma = 1.107$. Here, a good agreement is observed.

Let us note that if we consider this problem but with $l_3 = pl_1$, with an even integer p, the curve Σ_1 does not intersect Σ_2. As a result, the level spacing probability density is zero between $\Delta = 0$ and a value Δ_c. This is ilustrated in

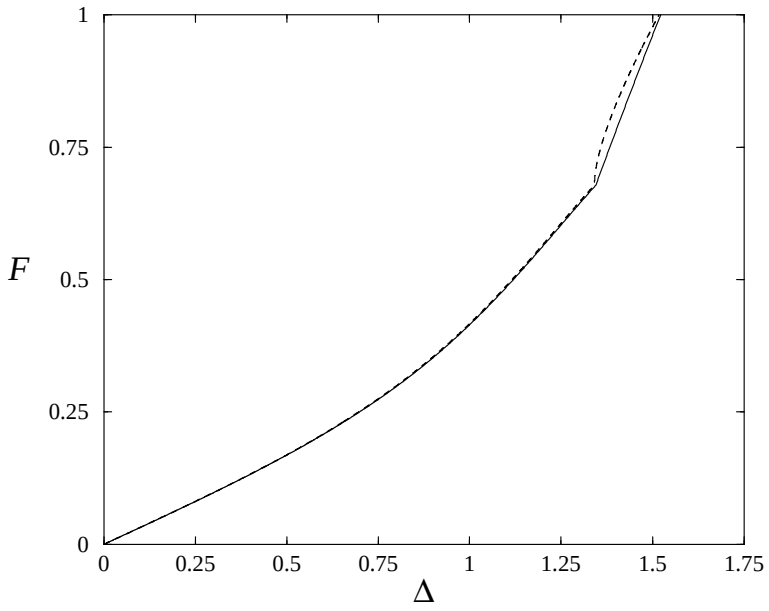

Figure 5: Cumulative function for the same graph as in Fig. 4. The solid line is the theoretical calculation done in the text and the dashed line is the numerical result.

Fig. 6 with $p = 2$.

5.3 Other simple graphs

Here, we study the level spacing in simple graphs with bonds connected to one vertex and thus forming a loop.

First, we consider the graph formed by two loops attached to a single vertex. This graph has the form of an eight. The zeros are determined by the function $f(k) = F(x_1 = l_1 k, x_2 = l_2 k)$ where

$$F(x_1, x_2) = (\cos x_2 - 1) \sin x_1 + (\cos x_1 - 1) \sin x_2 \tag{44}$$

This function is 2π-periodic in each variable and the surface Σ obtained by $F(x_1, x_2) = 0$ is considered in the torus $-\pi < x_1 < \pi$ and $-\pi < x_2 < \pi$. It is easy to see that this surface is composed by $\Sigma_1 = \{x_1 = 0, -\pi < x_2 < \pi\}$, $\Sigma_2 = \{x_2 = 0, -\pi < x_1 < \pi\}$ and $\Sigma_{12} = \{x_1 + x_2 = 0, -\pi < x_2 < \pi\}$. These three sheets intersect at the singular point $x_1 = x_2 = 0$. The function $F(x_1, x_2) = 0$ can thus be replaced by the cubic form $x_1 x_2 (x_1 + x_2) = 0$. The level spacing probability density can be written as

$$P(s) = \frac{\pi}{l_1 + l_2} \frac{1}{4\pi^2} \left\{ \int_{\Sigma_1} J_1 \; \delta[s - \tau_1(\xi)] \; d\xi + \int_{\Sigma_2} J_1 \; \delta[s - \tau_2(\xi)] \; d\xi + \int_{\Sigma_{12}} J_{12} \; \delta[s - \tau_{12}(\xi)] \; d\xi \right\}$$

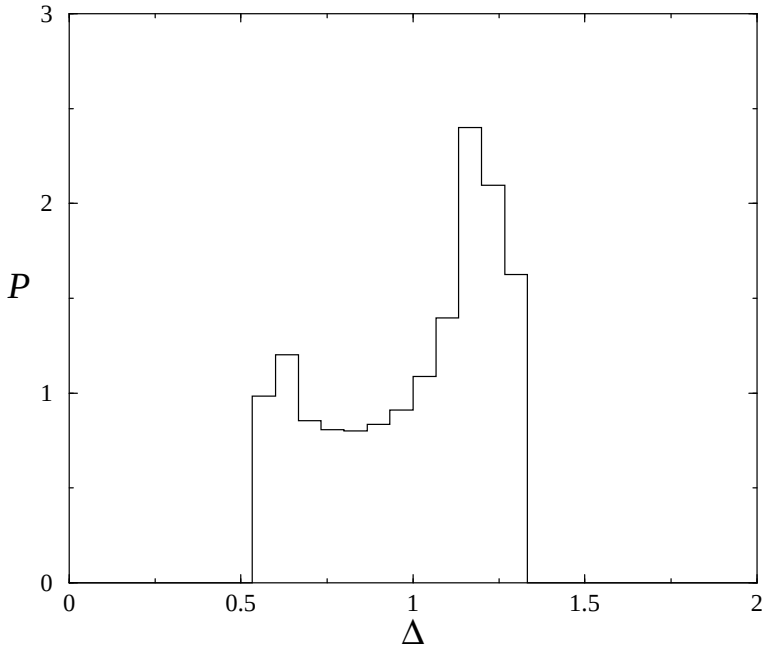

Figure 6: Here, we have considered $l_3 = 2l_1$ in the three-bond star graph to illustrate the existence of a critical value at which $P(\Delta)$ is different from zero. Here $l_1 = \sqrt{2}$ and $l_2 = \sqrt{3}$.

with $J_1 = l_1$, $J_2 = l_2$, $J_{12} = l_1 + l_2$, $\tau_1(\xi) = \tau_2(\xi) = \frac{\xi}{l_1+l_2}$ for $-\pi < \xi < 0$, $\tau_1(\xi) = \tau_2(\xi) = \frac{2\pi-\xi}{l_1+l_2}$ for $0 < \xi < \pi$, $\tau_{12}(\xi) = \frac{\xi}{l_1}$ for $0 < \xi < \frac{2\pi l_1}{l_1+l_2}$ and $\tau_{12}(\xi) = -\frac{\xi}{l_2}$ for $-\frac{2\pi l_2}{l_1+l_2} < \xi < 0$. Performing the integrals by using the variable $\Delta = \frac{l_1+l_2}{\pi}s$, we get

$$P(\Delta) = \begin{cases} \frac{1}{2}\,, & \text{if} \quad 0 < \Delta < 2 \\ 0\,, & \text{otherwise} \end{cases} \tag{45}$$

In this example, the spacing probability density $P(\Delta)$ is independent of the system parameters. We have confirmed this result with numerical calculations (data not shown).

Another graph of a similar type is the one composed by a bond and a loop attached to a vertex. This graph has the form of a nine. Here, the surface of section Σ is given by the equation

$$F(x_1, x_2) = 2\cos x_1 \cos x_2 - 2\cos x_1 - \sin x_1 \sin x_2 \tag{46}$$

The surface can be considered in the torus $-\pi/2 < x_1 < \pi/2$ and $-\pi < x_2 < \pi$ and it is given by

$$\begin{aligned}\Sigma_1 &= \{x_2 = 0, -\pi/2 < x_1 < \pi/2\} \\ \Sigma_2 &= \{\tan x_1 = 2(\cos x_2 - 1)/\sin x_2, -\pi < x_2 < \pi\}\end{aligned}$$

In this example, the calculation is similar to the one for the star graph with three bonds of two different lengths and we do not present it here. We only compute $P(\Delta)$ in the limit $\Delta \to 0$. For the small spacings, we can consider the quadratic form around the singularity at $(x_1 = 0, x_2 = 0)$ which is given by $F(x_1, x_2) \simeq x_1 x_2 + x_2^2$ for x_1, x_2 small enough. With this approximation the calculation is similar to the one of the previous graph. The result is $P(\Delta) \to \frac{l_2}{l_1+l_2}$ when $\Delta \to 0$.

5.4 Graphs with disconnected bonds

The formula (25) can be used to study the spacing distribution for the "integrable graphs" discussed in [5]. These graphs are obtained by imposing Dirichlet boundary conditions on the vertices and are called integrable because the classical dynamics in the graph correspond to a particle that bounces in a bond in a periodic motion which corresponds to a torus in phase space. In this case, the eigenvalues are obtained by the equations

$$\sin k l_b = 0 \ , \qquad \forall b \ ,$$

i.e.,

$$F(x_1, \ldots x_n) = \prod_{i=1}^{n} \sin x_i = 0$$

which is the equation for the surface Σ. This surface is composed of all the faces of the n-dimensional cube which defines the torus when we identify the corresponding boundaries, so that $\Sigma = \bigcup_i \Sigma_i$ with $\Sigma_i = \{x_i = 0, 0 < x_j < \pi \ , \quad \forall j \neq i\}$

In this case, the level spacing probability density (25) is given by

$$P(s) = \frac{\pi}{L_{\rm tot}} \frac{1}{\pi^n} \sum_k \int_{\Sigma_k} J_k \ \delta[s - \tau_k(s_k)] \ ds_k \tag{47}$$

where

$$\begin{aligned} J_k &= l_k \\ \text{and} \qquad \tau_k(s_k) &= \min_{j \neq k} \left\{ \frac{\pi - x_j^0}{l_j}, \frac{\pi}{l_k} \right\} \ . \end{aligned} \tag{48}$$

In the Appendix, we prove that Eq. (47) together with Eq. (48) are equivalent to:

$$P(\Delta) = \sum_{k=1}^{n}\sum_{j\neq k}^{n} \frac{l_k}{L_{\rm tot}}\frac{l_j}{L_{\rm tot}} \left[\prod_{i\neq j,k}^{n}\left(1-\frac{l_i}{L_{\rm tot}}\Delta\right)\right]\Theta\left(\frac{L_{\rm tot}}{l_1}-\Delta\right) + \frac{l_1}{L_{\rm tot}}\left[\prod_{i\neq 1}^{n}\left(1-\frac{l_i}{l_1}\right)\right]\delta\left(\Delta-\frac{L_{\rm tot}}{l_1}\right) \tag{49}$$

where l_1 is the largest length of the graph.

The distribution (49) is in general different from the Poisson distribution. The Poisson distribution is the limit of (49) when $\frac{l_1}{L_{\rm tot}} \to 0$. Indeed, in this limit, the delta peak vanishes, the Heaviside function equals one and, since $\sum l_i = L_{\rm tot}$, we find

$$P(\Delta) = \lim_{n\to\infty}\prod_{i=1}^{n}\left(1-\frac{l_i}{L_{\rm tot}}\Delta\right) = {\rm e}^{-\Delta}$$

Let us remark that this limit means that the number of bonds goes to infinity but the lengths are kept constant.

In Fig. (7), we plot the distribution (49) for different numbers of bonds. We observe that, for two bonds, the distribution is constant (except for the delta peak) and that, for three bonds, it decays linearly. In Fig. (8), we plot (49) and the numerical result for a graph of eight disconnected bonds. We observe the very nice agreement with the formula (49), as well as the convergence toward the Poisson distribution.

We want to comment on the deviations with respect to the Poisson distribution. First, we observe a maximum spacing which is easy to understand. The "regular" spectrum consists in a superposition of spectra $\left\{\pi\frac{n}{l_i}\right\}$ (*i.e.*, equally spaced levels). The largest spacing in this superposition is equal than the spacing $\frac{\pi}{l_1}$ where l_1 is the largest of the lengths l. In the scaled variable of unit mean spacing, this is $\frac{L_{\rm tot}}{l_1}$. This maximum spacing will appear repeatedly over the whole k-axis creating the delta peak in the distribution.

There is another interesting deviation with respect to the Poissonian distribution. We can see from (49) that the probability density of finding two levels in coincidence is $P(0) = 1 - \sum_i \frac{l_i^2}{L_{\rm tot}^2} < 1$. We can compute this probability in another way: Writing the level density $\rho(k)$ in the scaled variable x of unit mean spacing

$$\rho(x) = \sum_{j=1}^{n}\sum_{m=0}^{\infty}\delta\left(x-\frac{mL_{\rm tot}}{l_j}\right)$$

and using the Poisson formula for the Fourier transform, we obtain the "power spectrum"

$$\Pi(y) = \frac{1}{2\pi}\int_{-\infty}^{\infty} du\ {\rm e}^{iyu}\,\langle\tilde\rho(x)\tilde\rho(x+u)\rangle = \sum_{j=1}^{n}\sum_{m\neq 0}\frac{l_j^2}{L_{\rm tot}^2}\delta\left(y-2\pi\frac{l_j m}{L_{\rm tot}}\right)$$

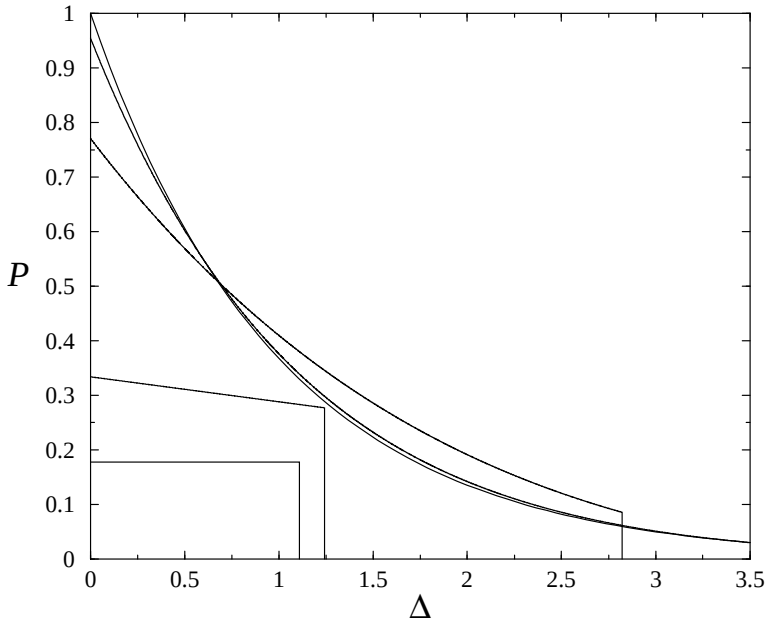

Figure 7: Theoretical level spacing distribution for graphs with disconnected bonds given by Eq. (49). Here, P means $P(\Delta)$. We have omitted the delta peak from the curves. The constant distribution is for the graph with 2 bonds. The linear distribution is for a graph with 3 bonds. Then, we plot the distributions for graphs with 8 bonds and with 30 bonds, respectively. The last one is close to the Poisson distribution that is also plotted but it starts at a smaller value as predicted from (49). The lengths are given by the formula $l_i = \sqrt{i}$ except for $l_1 = \sqrt{167}$, $l_4 = \sqrt{107}$, $l_8 = \exp(1)$, $l_9 = \sqrt{105}$, $l_{16} = \sqrt{119}$, and $l_{25} = \sqrt{134}$.

where $\langle\rangle$ is the average over x and $\tilde{\rho}$ represents the fluctuations of ρ around 1 (the mean density in this variable). Now, the mean number of levels in the interval $[x+\Delta, x+\Delta+d\Delta]$ given that there is a level at x is provided by $g(\Delta)d\Delta$ with [11]

$$g(\Delta) = 1 + \int_{-\infty}^{\infty} dy\ \mathrm{e}^{iy\Delta} \left[\Pi(y) - \frac{1}{2\pi}\right].$$

Thus, in the case of integrable graphs, we get

$$g(\Delta) = 1 - \sum_i \frac{l_i^2}{L_{\mathrm{tot}}^2} + \sum_{j=1}^{n} \sum_{m\neq 0} \delta\left(\Delta - \frac{mL_{\mathrm{tot}}}{l_j}\right).$$

We see that $g(0) = P(0)$. In order to compute the level spacing distribution, it is often assumed that $P(\Delta)$ is proportional to $g(\Delta)$ and that the levels are uncorrelated, so the probability of having two neighboring levels at a distance Δ

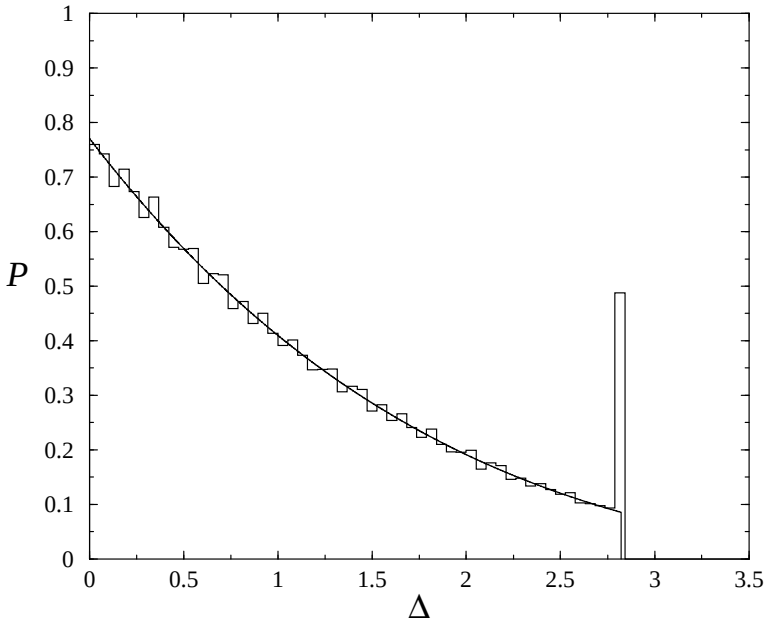

Figure 8: Numerical and theoretical level spacing probability densities for a graph with eigth disconnected bonds. Here, P means $P(\Delta)$. We have omitted the delta peak from the theoretical curve (49) but we see that its position coincides with the numerial peak. The histogram was built with 134050 spacings. The lengths are $l_1 = \sqrt{167}$, $l_2 = \sqrt{2}$, $l_3 = \sqrt{3}$, $l_4 = \sqrt{107}$, $l_5 = \sqrt{5}$, $l_6 = \sqrt{6}$, $l_7 = \sqrt{7}$, and $l_8 = \exp(1)$.

is given by $P(\Delta) = g(\Delta)\mathrm{e}^{-\int_0^\Delta g(x)dx}$ [11, 12]. We can see that these assumptions are not justified in the case of graphs but they are approximately valid for the very small spacings and also for the case of graphs with infinitely many bonds where the distribution is the Poisson distribution.

We have explored the dependence on the lengths of the bonds in the level spacing distribution (49). Figure 9 shows the deviations with respect to a Poisson distribution for two sets of lengths and the difference between them. We see that the dependence on the lengths for a graph of 10 lengths is very weak in the integrable case. We also observe in the figure that the deviations from the Poisson distribution is maximum for $\Delta = 0$.

6 Level spacing in complex graphs

We have computed the level spacing distribution for a fully connected pentagon. In figure 10 we depict the cumulative function obtained numerically with more than 100000 levels together with the RMT prediction[13]. Although the agree-

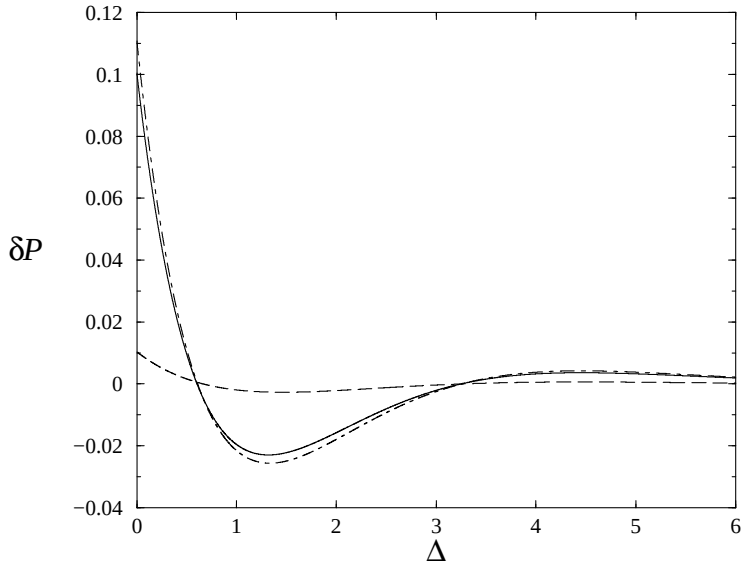

Figure 9: Deviations of Eq. (49) with respect to the Poisson distribution for for a graph with ten disconnected bonds. Here, $\delta P = \exp(-\Delta) - P(\Delta)$. The dot-dashed line is for the set of lengths $l_1 = \sqrt{3}$, $l_2 = \sqrt{5}$, $l_3 = \sqrt{7}$, $l_4 = \sqrt{11}$, $l_5 = \sqrt{13}$, $l_6 = \sqrt{17}$, $l_7 = \sqrt{19}$, $l_8 = \sqrt{23}$, $l_9 = \sqrt{29}$, $l_{10} = \sqrt{31}$. The solid line for the lengths $l_1 = \sqrt{101}$, $l_2 = \sqrt{103}$, $l_3 = \sqrt{107}$, $l_4 = \sqrt{109}$, $l_5 = \sqrt{113}$, $l_6 = \sqrt{127}$, $l_7 = \sqrt{131}$, $l_8 = \sqrt{137}$, $l_9 = \sqrt{139}$, $l_{10} = \sqrt{149}$. The long dashed line represents the difference between the densities evaluated with (49) in the two different cases.

ment is very good some systematic deviations exist. In figure 11 we plot these deviations for three different sets of lengths. We can see that they are very close to each other showing that the fluctuations are independent of the graph lengths. The dot-dashed line in figure 11 represents the fluctuations around RMT for a fully connected tetrahedron [5]. We can conclude from these results that the fluctuations around RMT depend on the topology of the graphs but does not depend much on their lengths. Moreover, we observe that the pentagon (a graph of 5 vertex, 10 bonds and valence 4) has bigger deviations with respect RMT than the tetrahedron (a graph of 4 vertex, 6 bonds and valence 3). This behavior is reminiscent of an observation in [5] that for a star graph of 15 bonds the form factor deviates more from RMT that for a star of 5 bonds (see also [9]). These results would suggest that the valence plays a role in the deviations with respect to RMT.

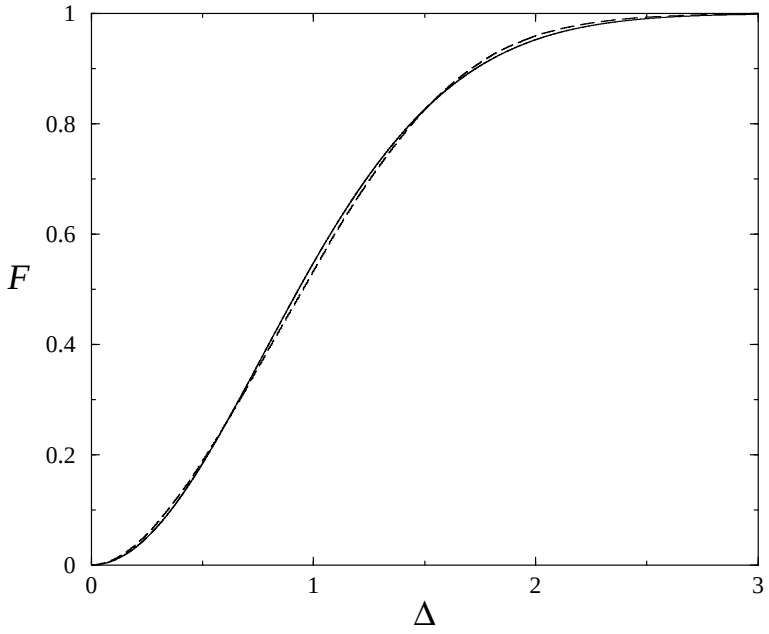

Figure 10: Cumulative function of the level spacing distribution for a fully connected pentagon. The dashed line is the numerical result for the pentagon with lengths $L_i = 0.6 l_i$ and $l_1 = \sqrt{2}$, $l_2 = \sqrt{3}$, $l_3 = \sqrt{5}$, $l_4 = \sqrt{6}$, $l_5 = \sqrt{7}$, $l_6 = \pi$, $l_7 = \exp(1)$, $l_8 = \sqrt{10}$, $l_9 = \sqrt{11}$, $l_{10} = \sqrt{13}$. The solid line is the RMT result.

7 Comparison with Berry's theory

Berry has studied the level spacing distribution in classically chaotic systems with a similar idea as the one we have developed here [10]. He noticed that, for a typical Hamiltonian with real eigenfunctions (which is the same situation as the one we consider here), it is necessary to vary two parameters in order for two levels to be degenerate. This is the content of a theorem originally due to von Neumann and Wigner. It also implies that, in the three-dimensional space of the two parameters A and B and of the energy E, the eigenvalue surface $E = E_{\pm}(A, B)$ has the form of a double cone with its sheets joined at the "diabolical point" (A^*, B^*, E^*), where A^*, B^* are the parameters for which the degeneracy occurs. Following Berry, these cones are distributed in the space (A, B, E) according to a unknown probability distribution $\rho(A, B, E)$. Berry has also considered a probability distribution which rules the geometry of the cones [$\pi(a, b, c)$ where a, b, c are the parameters in the quadratic form which defines the cone].

The level spacing probability distribution is given by the average (6) over energy, which can be considered in the semiclassical limit where infinitely many

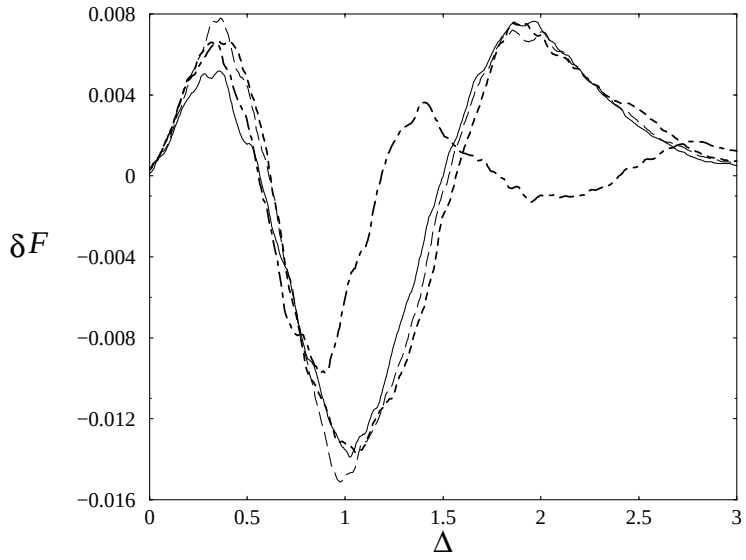

Figure 11: Deviations of the cumulative function of the spacing distribution for different complex graphs with respect to the RMT result: $\delta F = F - F_{RMT}$. The long dashed line represents this deviation for a fully conected pentagon with the same set of lengths as in figure 10. The dashed line represents this deviation for the lengths $L_i = 0.4 l_i$ with the l_i of the first set in figure 9 and the solid line for the lengths $L_i = 0.14 l_i$ with the l_i of the second set in figure 9. The dot-dashed line represents this fluctuations for a tetrahedron with the lengths $L_i = 1.05 l_i$ $l_1 = \sqrt{2}$, $l_2 = \sqrt{3}$, $l_3 = \pi$, $l_4 = \sqrt{6}$, $l_5 = \sqrt{7}$, $l_6 = \sqrt{13}$.

levels lie near any given E. As a consequence, the level spacing is given for small spacings by the successive crossings of the conical surfaces with the line $(E, A = A_0, B = B_0)$ where A_0 and B_0 are the parameters of the actual Hamiltonian under study. Berry argues that, since there is nothing special about the system with the parameters (A_0, B_0), the energy average can be augmented by an ensemble average over a region (A, B) near (A_0, B_0). Whereupon, the level spacing becomes

$$P(\Delta) = \frac{\rho(A_0, B_0, E)}{\langle d(E) \rangle} \int da\, db\, dc\, \pi(a, b, c) \int dA\, dB\, \delta(\Delta - \sqrt{aA^2 + 2bAB + cB^2})$$

After the change of variables $\alpha = A/\Delta$, $\beta = B/\Delta$, the previous equation gives

$$P(\Delta) \sim \Delta$$

where the proportionality factor involves a geometric average. Berry's argument shows that the level spacing density should vanish linearly in generic systems because of the level repulsion, as expected from random matrix theory.

The main difference between Berry's derivation and our derivation is that he introduces by hand the ensemble average. In our derivation, the ensemble average naturally appears from a rigorous equivalence between the energy average and the ensemble average given by the ergodic theorem. This ensemble average introduced by ergodicity has the advantage of keeping all the specificities of the system, *i.e.*, the dependence on the lengths of the graph. We expect that these specificities disappear for graphs which are sufficiently large, in a way which has still to be understood for graphs with connected bonds.

8 Conclusions and discussion

In this article, we have derived a formula for the spacing probability distribution of the energy levels of quantum graphs and, more generally, for systems where the secular equation is given by an almost-periodic function. Our formula is based on the ergodic properties of a continuous-time dynamical system defined on a torus. This ergodic flow induces a Poincaré map in a certain surface of section which corresponds to the locus of the energy eigenvalues in the phase space of the flow. The level spacings are explicitly related to the times of first return in the surface of section. The level spacing distribution is thus given by the distribution of the first-return times of the ergodic flow in the Poincaré surface of section.

We have applied this formula to different graphs. In general, the slope of the spacing density $P(\Delta)$ at $\Delta = 0$ depends on the system parameters and we have been able to calculate explicitly this dependence in several graphs.

We have also studied in detail the "regular" spectrum of integrable graphs. One important application of our formula (25) is the following

Theorem:

If the bonds of the graph are disconnected so that the spectrum is a superposition of n independent equally spaced spectra of wavenumbers and if the bond lengths are mutually incommensurable, the level spacing probability distribution is exactly given by Eq. (49) when the distribution is expressed in the variable where the level density is equal to one. The distribution (49) converges to the Poisson distribution in the limit $n \to \infty$.

On the other hand, for large connected graphs, the level spacing distribution is close to the Dyson-Gaudin-Mehta spacing distribution of RMT although deviations are numerically observed which depend mainly on the topology of the quantum graph. The deviations with respect to RMT are more important for smaller graphs than for larger graphs but the effect of Wigner repulsion is still present in very small graphs where we observe that the spacing density also vanishes linearly like $P(\Delta) \sim \Delta$.

The different results we have obtained can be understood on the basis of the general properties of the surface of section Σ, which plays a particularly important role. First of all, we remark that the surface Σ is defined as the set of the zeros of $f(k) = F(kl_1, ..., kl_n) = 0$ in the n-dimensional phase space $(x_1 = kl_1, ..., x_n = kl_n)$ of the ergodic flow. Therefore, the surface Σ is of di-

mension $n-1$ in this space. According to the von Neumann-Wigner theorem, two zeros are generically degenerate only if two constraints are imposed on the parameters of the systems which are here the lengths l_i of the bonds. Consequently, the dimension of the subset of these degeneracies is $n-3$, generically. In the following, we refer to this subset as the singular manifold.

The aforementioned generic situation is already encountered in graphs with three incommensurate lengths for which the phase space of the ergodic flow is of dimension $n=3$, the surface of section Σ of dimension $n-1=2$, and the degeneracy subset of dimension $n-3=0$. Indeed, in the example of Subsection 5.1, the surface Σ forms a cone with a self-intersection at a point. This example shows that a spacing density vanishing linearly is generically possible as soon as there are three incommensurate lengths.

However, for graphs with only two incommensurate bond lengths, only two behaviors are generic: either (1) $P(0)\neq 0$ or (2) $P(\Delta)=0$ for $0<\Delta<\Delta_c$. For such graphs, the torus is two-dimensional and the surface giving the eigenvalue is one-dimensional, *i.e.*, a line on the torus. Generically, this line may intersect itself leading to the case (1), or it may have no intersection leading to the case (2). Therefore, generically, we should not expect a spacing density which vanishes linearly like $P(\Delta)\sim\Delta$ for a graph with only two incommensurate lengths. This result is illustrated with the examples of Subsections 5.2 and 5.3.

In the two dimensional examples, we notice that the singular manifold has the dimension $n-2$ and is a point on a two-dimensional torus and, as a corollary, $P(\Delta)$ starts with a finite value. This last result is supported by the fact that, for the non-generic integrable systems, two levels can come in degeneracy by varying only one parameter. Indeed, the singular manifold is of dimension $n-2$ for the disconnected "integrable graphs" because the surface Σ is composed by the faces of the cube and their intersections are of dimension $n-2$, as we saw in Subsection 5.4. This discusion shows that the graphs with two incommensurate lengths belong to a non-generic class because the singular manifold can never be of dimension $n-3$ for $n=2$. It is important to notice that this statement does not contradict Berry's theory because he considers general Hamiltonian systems where the levels are given by an equation like $\tilde{f}(k,l_1,l_2)=0$ (if we call l_1 and l_2 the two parameters that enter in his theory) which allows the existence of a cone in the (k,l_1,l_2) space, while, for graphs with two incommensurate lengths, the secular equation has the special form $\tilde{f}(k,l_1,l_2)=f(kl_1,kl_2)=0$ which does not allow the existence of such a cone.

In summary, the important point which makes the difference in the behavior of $P(\Delta)$ at small spacings Δ is the dimension of the singular manifold which is $n-3$ for the repulsion and a distribution as $P(\Delta)\sim\Delta$, but $n-2$ for the clustering and a distribution as $P(\Delta)\sim$ constant.

We notice that the degree of the polynomial that describes the surface around the singular point seems to be not essential for this matter because we have repulsion and clustering for cases where the surface around the singular point is given by a quadratic form [see Subsection 5.1 Subsection 5.2 and Eq. (46)]. We have also seen an example with clustering [see Eq. (44)] where the surface is described by a cubic form.

We have not commented on the topology of the singular manifold. It can happen that the intersection of two surfaces is transverse or tangent and this will influence the behavior of $P(\Delta)$ near $\Delta = 0$. In all the examples that we consider, the intersection is transverse which is the generic case when there is no restriction on the kind of surface.

Several extensions of this work are possible. We may wonder which are the generic properties of the surface Σ and the function $\tau(\xi)$ for typical graphs and apply the formula (25) to such generic situations. We notice that there are some restrictions on Σ. In particular, the number of sheets with projection in a given direction depends on the number of bonds with lengths associated with this direction, as we have seen in Section 4. There can be other restrictions as a consequence of the properties of the Hamiltonian (hermiticity, etc). In this problem, a difficulty comes from the fact that the dimension of the torus is equal to the number of incommensurate lengths in the graph. This makes difficult the study of complex graphs. Another possible direction is the study of perturbations of integrable graphs. Such perturbations are expected to deform the surface Σ and we may investigate the transition from our quasi-Poissonian distribution (49) to the RMT distribution.

Since the graphs of the kind that we have discussed here have been used to model transport in mesoscopic systems, our work can find interesting applications in this context.

Appendix

Here, we derive Eq. (49) from Eq. (47). The strategy is to divide the surfaces Σ_k into regions where the minimum, which appears in the definition (48) of $\tau_k(s_k)$, takes a given form. We call $\mathcal{R}_j^k$ the region where $\tau_k(s_k) = \frac{\pi - x_j^0}{l_j}$ with $j \neq k$ and $\mathcal{R}_k^k$ the region where $\tau_k(s_k) = \frac{\pi}{l_k}$.

First, we compute

$$\int_{\Sigma_1} ds_1 \; \delta[s - \tau_1(s_1)] = \int_0^\pi dx_2^0 \cdots \int_0^\pi dx_n^0 \; \delta[s - \tau_1(x_2^0, \ldots, x_n^0)]$$

with $\tau_1(s_1) = \min_{j \neq 1} \left\{ \frac{\pi - x_j^0}{l_j}, \frac{\pi}{l_1} \right\}$.

Consider the flow (8) introduced in Section 3:

$$\begin{aligned} x_1 &= l_1 t \\ x_i &= l_i t + x_i^0 \; , \qquad i = 2, \ldots, n \end{aligned} \tag{50}$$

We look after any region in the surface Σ_1 where $\tau_1(x_2^0, \ldots, x_n^0) = \frac{\pi}{l_1}$. To determine these regions, we replace t by $\frac{\pi}{l_1}$ in (50). This region should satisfy the following inequalities

$$0 < x_i = l_i \frac{\pi}{l_1} + x_i^0 < \pi \; , \qquad i = 2, \ldots, n \tag{51}$$

which express the fact that the trajectory did not cross any boundary of the torus before arriving at $x_1 = \pi$.

From (51), we get that the region $\mathcal{R}_1^1$ where $\tau_1(s_1) = \frac{\pi}{l_1}$ is given by

$$0 < x_i^0 < \pi \left(1 - \frac{l_i}{l_1}\right) \ , \qquad i = 2, \ldots, n \tag{52}$$

We note that this result gives a border for all the other regions

$$x_i^0 > \pi \left(1 - \frac{l_i}{l_1}\right) \ , \qquad i = 2, \ldots, n \ . \tag{53}$$

Now, we look for the regions where $\tau_1(s_1) = \frac{\pi - x_j^0}{l_j}$, $\forall j \neq 1$. Again, from the substitution of this expression in Eq. (50), we obtain the following inequalities

$$\begin{aligned} 0 < x_1 &= \frac{l_1}{l_j}(\pi - x_j^0) < \pi \\ 0 < x_i &= \frac{l_i}{l_j}(\pi - x_j^0) + x_i^0 < \pi \ , \qquad i = 2, \ldots, n, \quad i \neq k \end{aligned}$$

These inequalities imply that

$$\begin{aligned} \pi \left(1 - \frac{l_j}{l_1}\right) < \quad x_j^0 \quad &< \pi \ , \qquad j \neq 1 \\ 0 < \quad x_m^0 \quad &< \pi - \frac{l_m}{l_j}(\pi - x_j^0) \ , \qquad\qquad m \neq \{1, j\} \end{aligned} \tag{54}$$

is the region $\mathcal{R}_j^1$ where $\tau_1(s_1) = \frac{\pi - x_j^0}{l_j}$.

The union of $\mathcal{R}_1^1$ given by (52) with $\mathcal{R}_j^1$ ($\forall j \neq 1$) given by (54) is equal to Σ_1.

Thus, we have that

$$\begin{aligned} \int_{\Sigma_1} ds_1 \ \delta[s - \tau_1(s_1)] \quad &= \quad \left[\prod_{i \neq 1}^{n} \int_0^{\pi\left(1 - \frac{l_i}{l_1}\right)} dx_i^0\right] \delta\left(s - \frac{\pi}{l_1}\right) \\ &+ \quad \sum_{j \neq 1} \int_{\pi\left(1 - \frac{l_j}{l_1}\right)}^{\pi} dx_j^0 \prod_{i \neq \{1,j\}}^{n} \int_0^{\pi\left(1 - \frac{l_i}{l_1}\right)} dx_i^0 \ \delta\left(s - \frac{\pi - x_j^0}{l_j}\right) \ . \end{aligned} \tag{55}$$

The first term represents the integration over $\mathcal{R}_1^1$ and the second term the integration over $\mathcal{R}_j^1$. The explicit evaluation gives:

$$\int_{\Sigma_1} ds_1 \ \delta[s - \tau_1(s_1)] = \pi^{n-1} \left[\prod_{i \neq 1}^{n} \left(1 - \frac{l_i}{l_1}\right)\right] \delta\left(s - \frac{\pi}{l_1}\right) + \sum_{j \neq 1} l_j \left[\prod_{i \neq \{1,j\}}^{n} (\pi - l_i s)\right] \Theta\left(\frac{\pi}{l_1} - s\right) \tag{56}$$

Now, we compute

$$\int_{\Sigma_k} ds_k\ \delta[s-\tau_k(s_k)] = \int_0^\pi dx_1^0 \cdots \int_0^\pi dx_{k-1}^0 \int_0^\pi dx_{k+1}^0 \cdots \int_0^\pi dx_n^0\ \delta[s-\tau_k(x_1^0,\ldots,x_{k-1}^0,x_{k+1}^0,\ldots,x_n^0)] \tag{57}$$

As before, we consider the flow

$$\begin{aligned} x_k &= l_k t \\ x_i &= l_i t + x_i^0\ , \qquad i=1,\ldots,n, \quad i\neq k \end{aligned} \tag{58}$$

It is easy to see that there is no region where $\tau_k(s_k)=\frac{\pi}{l_k}$. This is due to the fact that the existence of such a region requires $\frac{l_1}{l_k}\pi + x_1^0 < \pi$ and, because $l_1 > l_k$, there is no positive value of x_1^0 where this inequality holds.

Now, we look for the regions $\mathcal{R}_j^k$ where $\tau_k(s_k)=\frac{\pi-x_j^0}{l_j}$. Replacing this $\tau_k(s_k)$ in (58) we get the following conditions

$$\begin{aligned} 0<x_k &= \frac{l_k}{l_j}(\pi-x_j^0)<\pi \\ 0<x_i &= \frac{l_i}{l_j}(\pi-x_j^0)+x_i^0<\pi\ , \qquad i=1,\ldots,n, \quad i\neq k \end{aligned} \tag{59}$$

These conditions are satisfied only in the region $\mathcal{R}_j^k$ where $\tau_k(s_k)=\frac{\pi-x_j^0}{l_j}$ and which is defined by

$$\pi\left(1-\frac{l_j}{l_1}\right) < \quad x_j^0 \quad < \pi \tag{60}$$

$$0 < \quad x_m^0 \quad < \pi - \frac{l_m}{l_j}(\pi-x_j^0)\ , \qquad m\neq\{j,k\}\ . \tag{61}$$

Again, the union of the regions $\mathcal{R}_j^k$ gives Σ_k. Note that these regions are outside the border given by (53) as one expected.

Thus, one has

$$\int_{\Sigma_k} ds_k\ \delta[s-\tau_k(s_k)] = \sum_{j\neq k}\int_{\pi\left(1-\frac{l_j}{l_1}\right)}^{\pi} \prod_{m\neq\{j,k\}}^{n} \int_0^{\pi-\frac{l_m}{l_j}(\pi-x_j^0)} dx_m^0\ \delta\left(s-\frac{\pi-x_j^0}{l_j}\right) \tag{62}$$

or more explicitly

$$\int_{\Sigma_k} ds_k\ \delta[s-\tau_k(s_k)] = \sum_{j\neq k}^{n} l_j \left[\prod_{i\neq\{j,k\}}^{n}(\pi-l_i s)\right]\Theta\left(\frac{\pi}{l_1}-s\right) \tag{63}$$

Finally, we substitute the results (56) and (63) in (47) and we get

$$P(s) = \frac{l_1}{L_{\rm tot}} \left[\prod_{i \neq 1}^{n} \left(1 - \frac{l_i}{l_1} \right) \right] \delta \left(s - \frac{\pi}{l_1} \right) + \frac{1}{\pi^{n-1} L_{\rm tot}} \sum_{k=1}^{n} \sum_{j \neq k}^{n} l_j l_k \left[\prod_{i \neq \{j,k\}}^{n} (\pi - l_i s) \right] \Theta \left(\frac{\pi}{l_1} - s \right) \tag{64}$$

which gives Eq. (49) when written in terms of the variable $\Delta = \frac{L_{\rm tot}}{\pi} s$.

Acknowledgements. We dedicate this work to Professor Grégoire Nicolis on the occasion of his sixtieth birthday and we thank him for support and encouragement in this research. F. B. is financially supported by the "Communauté française de Belgique" and P. G. by the National Fund for Scientific Research (F. N. R. S. Belgium). This work is supported, in part, by the Interuniversity Attraction Pole program of the Belgian Federal Office of Scientific, Technical and Cultural Affairs, by the Training and Mobility Program of the European Commission, and by the F. N. R. S. .

References

[1] O. Bohigas, in: M.-J. Giannoni, A. Voros, and J. Zinn-Justin, Eds., *Chaos and Quantum Physics* (North-Holland, Amsterdam, 1991) pp. 87-199.

[2] M. G. Gutzwiller, *Chaos in Classical and Quantum Mechanics*, Interdisciplinary Applied Mathematics Vol I, edited by F. John (Springer-Verlag, New York, 1990).

[3] M. V. Berry, Proc. R. Soc. London A **400**, 229 (1985).

[4] T. Kottos and U. Smilansky, Phys. Rev. Lett **79**, 4794(1998).

[5] T. Kottos and U. Smilansky, Annals of Physics **273**, 1 (1999).

[6] T. Kottos and U. Smilansky, Preprint "Chaotic Scattering on Graphs", chao-dyn/9906008.

[7] H. Schanz and U. Smilansky, Preprint "Periodic-Orbit Theory of Anderson Localization on Graphs", chao-dyn/9909023.

[8] H. Schanz and U. Smilansky, Proc. Australian Summer School in Quantum Chaos and Mesoscopics (Canberra), Preprint "Spectral Statistics for Quantum Graphs: Periodic Orbits and Combinatorics", chao-dyn/9904007.

[9] G. Berkolaiko and J. P. Keating, J. Phys. A **32**, 7827 (1999).

[10] M. V. Berry, in: G. Iooss, R. H. G. Helleman and R. Stora, Eds., *Chaotic Behavior of Deterministic Systems*, (North-Holland, Amsterdam,1983) pp.171-271.

[11] M. V. Berry and M. Tabor, Proc. R. Soc. London A **356**, 375 (1977).

[12] C. E. Porter, *Statistical Theories of Spectra: Fluctuations* (Academic Press, New-York & London, 1965).

[13] F.Haake, *Quantum Signatures of Chaos* (Springer-Verlag, Berlin, 1991).